

Technical Report

Suppression of the Malignant Phenotype in Pancreatic Cancer by Overexpression of Phospholipid Hydroperoxide Glutathione Peroxidase

JINGRU LIU,¹ JUAN DU,¹ YUPING ZHANG,¹ WENQING SUN,¹ BRIAN J. SMITH,²
LARRY W. OBERLEY,^{1,2} and JOSEPH J. CULLEN¹⁻⁴

ABSTRACT

Phospholipid glutathione peroxidase (PhGPx) reduces lipid hydroperoxides generated in biomembranes and also uses a wide range of reducing cofactors in addition to glutathione. PhGPx is synthesized as a mitochondrial PhGPx form (L-form) and as a nonmitochondrial PhGPx form (S-form). Our aims were to determine whether overexpression of PhGPx altered pancreatic tumor cell behavior. Pancreatic cancer cell lines were found by Western blotting to have diminished levels of PhGPx-immunoreactive protein compared with normal human pancreas. To normalize the levels of this protein, PhGPx was overexpressed in MIA PaCa-2 and AsPC-1 human pancreatic cancer cells by infection with an adenovirus–PhGPx L-form construct (*AdPhGPx-L-form*) (0–200 MOI) or with an adenovirus–PhGPx S-form construct (*AdPhGPx-S-form*) (0–200 MOI), and cell growth, plating efficiency, and growth in soft agar were determined. Pancreatic cancer cells were also injected subcutaneously into nude mice and tumor volume was calculated. Single direct injections of the adenoviral–PhGPx constructs were made into preestablished tumors. *In vitro*, *AdPhGPx-S-form* demonstrated 80% tumor growth inhibition, whereas *AdPhGPx-L-form* demonstrated 95% tumor growth inhibition. *AdPhGPx-L-form* or *AdPhGPx-S-form* also decreased plating efficiency and growth in soft agar. *AdPhGPx-L-form* decreased *in vivo* tumor growth to a greater extent than did *AdPhGPx-S-form*. Because of the growth-inhibitory effects of PhGPx, lipid hydroperoxides may play an important role in the growth of pancreatic cancer.

INTRODUCTION

PANCREATIC CANCER, the fourth leading cause of cancer death in the United States, is one of the most aggressive malignancies (Jemal *et al.*, 2004). Surgical resection of the primary tumor remains the only potentially curative treatment for pancreatic cancer; however, in population-based studies the number of patients undergoing resection with curative intent can be less than 3% (Bramhall *et al.*, 1995). Other adjuvant treatments have not improved long-term survival, with the rate of chemotherapeutic response and radiotherapy response between

10 and 20% (White *et al.*, 1999). Because of the poor therapeutic responsiveness of pancreatic cancer to surgery, chemotherapy, and radiation therapy, survival beyond 5 years is rare (Yeo and Cameron, 1999). Thus, effective therapies for pancreatic cancer are needed to control progression and metastatic disease.

Our group demonstrated that glutathione peroxidase (GPx), which plays a key role not only in metabolizing H₂O₂, but also in catalyzing organic hydroperoxide removal, inhibits pancreatic cancer cell proliferation. In human pancreatic cancer cells, overexpression of glutathione peroxidase-1 (GPx1) by means of

¹Department of Radiation Oncology, University of Iowa College of Medicine, Iowa City, IA 52242.

²Holden Comprehensive Cancer Center, Iowa City, IA 52242.

³Department of Surgery, University of Iowa College of Medicine, Iowa City, IA 52242.

⁴Veterans Affairs Medical Center, Iowa City, IA 52242.

an adenoviral vector carrying the *GPx1* gene (*AdGPx1*) slowed cell growth and decreased plating efficiency and growth in soft agar, whereas the combination of *AdGPx1* and an adenoviral vector carrying the manganese superoxide dismutase gene (*AdMnSOD*) had the greatest effect on pancreatic tumor cell growth suppression (Liu *et al.*, 2004). *In vivo*, either *AdGPx1* or *AdMnSOD* alone slowed pancreatic tumor growth in nude mice, whereas the combination of *AdGPx1* and *AdMnSOD* potentiated tumor growth suppression and increased animal survival. These data suggest that hydroperoxides play an important role in pancreatic cancer cell proliferation.

Two members of the GPx family, GPx1 and phospholipid glutathione peroxidase (PhGPx), have been widely studied in relation to antioxidant cytoprotection and lipoxygenase regulation. GPx1 and PhGPx both contain the rare amino acid selenium (Se)-cysteine at the active site, and the active selenocysteine residue participates in the two-electron reduction of peroxides to alcohols. However, the two enzymes differ in functional size, subcellular distribution, and amino acid sequence (Ursini *et al.*, 1997). They also exhibit striking differences in peroxide reactivity: GPx1, an 85-kDa tetramer, is a major enzyme responsible for removing H₂O₂ and organic hydroperoxides. Under normal conditions peroxidized lipids are reduced by GPx1, which acts at low efficiency on membrane-bound lipid peroxides and only after their removal from the membrane by phospholipases. In contrast, PhGPx, a 20-kDa monomer, is the only known intracellular antioxidant enzyme that can directly reduce peroxidized phospholipid and cholesterol in membranes and can also use a wide range of reducing cofactors in addition to glutathione (Aumann *et al.*, 1997). The ability of PhGPx to reduce lipid hydroperoxides is thought to contribute to the enzymatic defenses against oxidative damage to the mitochondrial membrane (Imai and Nakagawa, 2003). PhGPx is synthesized as a long form, highly expressed in mitochondria, and as a short form that is expressed in nuclei, endoplasmic reticulum, and cytosol, but not in mitochondria (Sunde *et al.*, 1993).

The aims of our study were to determine whether lipid hydroperoxides play a role in growth of pancreatic cancer and whether overexpression of PhGPx alters tumor cell behavior. Our data demonstrated that PhGPx protein was decreased in pancreatic cancer cell lines when compared with normal human pancreas and that overexpression of PhGPx slowed tumor growth both *in vitro* and *in vivo*.

MATERIALS AND METHODS

Human pancreas

Human pancreatic specimens were retrieved from neurologically devastated, heart-beating patients who were transplant donors, but whose pancreas was considered unsuitable for transplantation or for which no recipient was available. Pancreatic specimens were discarded and not used in this study if the donor had any history of pancreatic disease. All specimens were retrieved at the University of Iowa Hospitals and Clinics (Iowa City, IA). The protocol to use human pancreatic specimens was approved by the University of Iowa Institutional Review Board for Human Subjects on February 12, 2001.

Cell culture

MIA PaCa-2 and Panc-1 cells are human primary pancreatic undifferentiated adenocarcinoma cells of ductal epithelial cell origin. The cells were maintained at 37°C in Dulbecco's modified Eagle's medium (DMEM; Invitrogen GIBCO, Grand Island, NY) supplemented with 10% heat-inactivated fetal bovine serum and 2.5% horse serum. AsPC-1 cells are poorly to moderately differentiated human pancreatic adenocarcinoma cells of ductal epithelial cell origin. AsPC-1 cells were maintained at 37°C in RPMI 1640 with 20% heat-inactivated fetal bovine serum. BxPC-3 cells are poorly differentiated human pancreatic adenocarcinoma cells and were maintained in RPMI 1640 with 10% fetal bovine serum. All cell lines were purchased from the American Type Culture Collection (Manassas, VA) and medium was obtained from Invitrogen GIBCO. All lines were regularly tested for mycoplasma and used only if mycoplasma negative.

Gene transfer by adenovirus

The adenoviral constructs used were based on replication-defective, E1- and partial E3-deleted recombinant adenovirus (Lam *et al.*, 1997). Inserted into the E1 region of the adenovirus genome was the human *PhGPx* or *MnSOD* gene, both driven by a cytomegalovirus promoter. To control for adenovirus we used adenovirus carrying no added DNA (*AdBgIII*). The adenoviral constructs were obtained from the University of Iowa Gene Transfer Vector Core (Iowa City, IA) or from ViraQuest (North Liberty, IA). The *AdMnSOD* construct was originally prepared by J. Engelhardt (University of Iowa, Iowa City, IA) (Zwacka *et al.*, 1998), and the *AdPhGPx* construct was produced by ViraQuest.

Approximately 10⁶ MIA PaCa-2 or AsPC-1 cells were plated in 10 ml of complete medium in a 90-cm² plastic dish and allowed to attach for 24 hr. Cells were then washed three times in serum- and antibiotic-free medium. The *AdPhGPx-L-form*, *AdPhGPx-S-form*, or *AdMnSOD* construct, suspended in 3% sucrose, was then applied to cells suspended in 4 ml of antibiotic-free medium at 0, 50, 100, and 200 multiplicities of infection (MOIs). Control cells were treated with 100 or 200 MOI of the *AdBgIII* construct. Cells were incubated with the adenoviral constructs for 24 hr. Medium was then replaced with 4 ml of complete medium.

Cell homogenization and protein determination

Cells were washed three times in phosphate-buffered saline (PBS, pH 7.0), scraped from the dishes with a rubber policeman, and then collected in potassium phosphate buffer (pH 7.8). This was followed by sonic disruption on ice for 30 sec in 10-sec bursts, using a sonic dismembrator with a cup horn (Fisher Scientific, Itasca, IL) at 100% power. Protein concentration was determined with a Bradford dye-binding protein assay kit (Bio-Rad, Hercules, CA) according to the manufacturer's instructions.

Western immunoblot analysis

Immunoreactive protein corresponding to MnSOD and PhGPx was identified and quantitated from total cell protein by the specific reaction of the immobilized protein with its antibody. To-

tal protein was electrophoresed in a 10% sodium dodecyl sulfate (SDS)-polyacrylamide running gel and a 5% stacking gel. β -Actin was used to determine equal loading. After transfer, gels were stained for protein loading with Coomassie blue to verify equal loading and the membranes were then blocked at room temperature for 1 hr in blocking solution (TTBS: 10 mM Tris-HCl, 150 mM NaCl [pH 8.0], 0.05% Tween 20, and 5% nonfat dried milk). To detect specific proteins, the membrane was incubated with specific antibody. After incubation with a 1:1000 dilution of primary antibody to MnSOD prepared and characterized in our laboratory (Oberley *et al.*, 1990), or with a 1:2000 dilution of primary antibody to PhGPx (LabFrontier, Seoul, South Korea), membranes were incubated with horseradish peroxidase-conjugated goat anti-rabbit IgG (diluted 1:10,000; Sigma, St. Louis, MO) at room temperature for 1 hr. Protein bands were visualized with an enhanced chemiluminescence (ECL) detection system (GE Healthcare, Piscataway, NJ). Western blots were performed at least twice.

Cell growth

Cells (1×10^4) were plated in 3 ml of complete medium in 6-well plates. Cells were trypsinized and then counted on alternate days for 1 to 2 weeks, using a Coulter counter (Beckman Coulter, Fullerton, CA). Cell population doubling time in hours (DT) was determined by the following equation:

$$DT \text{ (hours)} = 0.693(t - t_0) / \ln(N_t/N_0)$$

where t_0 is the time at which exponential growth began, t is time in hours, N_t is the cell number at time t , and N_0 is initial cell number (Aumann *et al.*, 1997). The adenoviral constructs used in the cell growth, plating efficiency, and growth in soft agar experiments expressed only one antioxidant protein. In the cell growth, plating efficiency, and soft agar growth experiments in which we used two adenoviral constructs, the AdBgIII vector was given to equalize the viral load of the combined viruses. Thus, AdBgIII was delivered as 200 MOI and the other

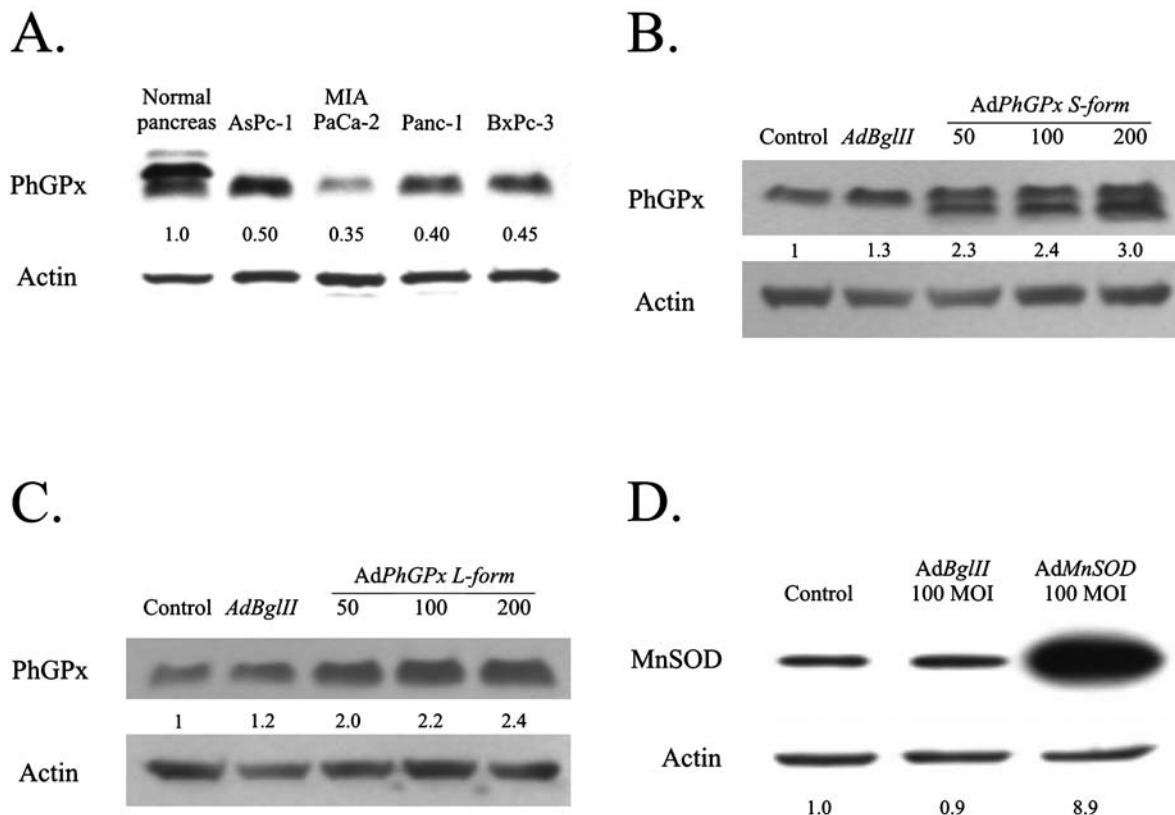
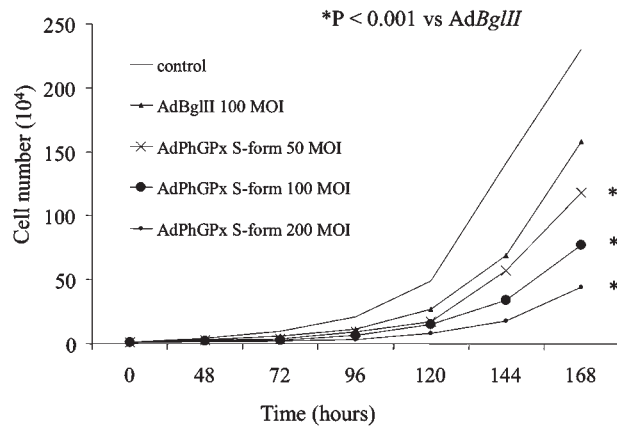
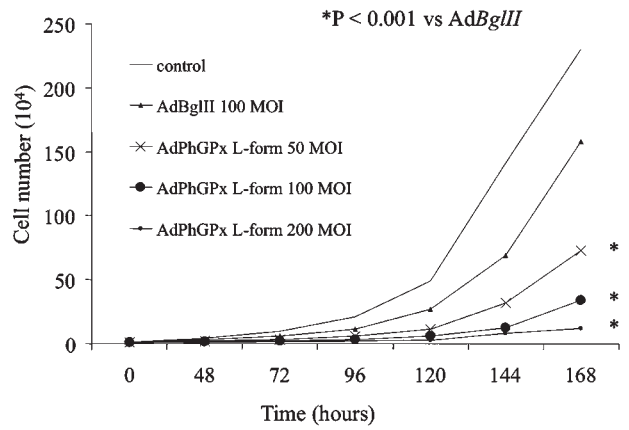


FIG. 1. (A) Western blot analysis of PhGPx in human pancreas and in the pancreatic cancer cell lines AsPC-1, MIA PaCa-2, Panc-1, and BxPC-3. Total protein was electrophoresed in a 12.5% SDS-polyacrylamide running gel and a 5% stacking gel. After blocking for 1 hr in TTBS containing 5% milk, the sheets were washed and then treated with rabbit anti-PhGPx polyclonal antibody. The area of the bands relative to human pancreas cells as measured by densitometric analysis is shown at the bottom of the lanes; these numbers indicate the relative amount of immunoreactive protein. Blots were repeated with similar results. (B) MIA PaCa-2 cells transduced with 200 MOI of AdBgIII or 0 to 200 MOI of AdPhGPx-S-form demonstrate increases in PhGPx immunoreactivity with increasing viral titer. No difference was seen with AdBgIII transfer (100 MOI) compared with parental cells. The area of the bands relative to MIA PaCa-2 (control) cells as measured by densitometric analysis is shown at the bottom of the lanes; these numbers indicate the relative amount of protein. All immunoblots were repeated to confirm the findings. (C) MIA PaCa-2 cells transduced with 200 MOI of AdBgIII or 0 to 200 MOI of AdPhGPx-L-form demonstrate increases in PhGPx immunoreactivity with increasing viral titer. No difference was seen between cells treated with 100 MOI of AdBgIII and parental cells. (D) MIA PaCa-2 cells transduced with 100 MOI of AdBgIII or 100 MOI of AdMnSOD demonstrate increases in MnSOD immunoreactivity. No difference was seen between cells treated with 100 MOI of AdBgIII and parental cells.

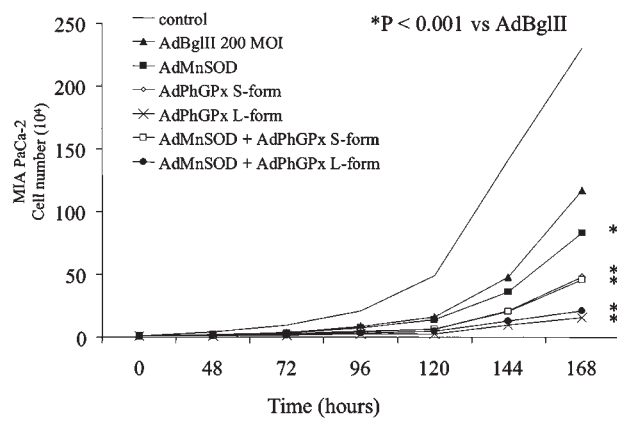
A.



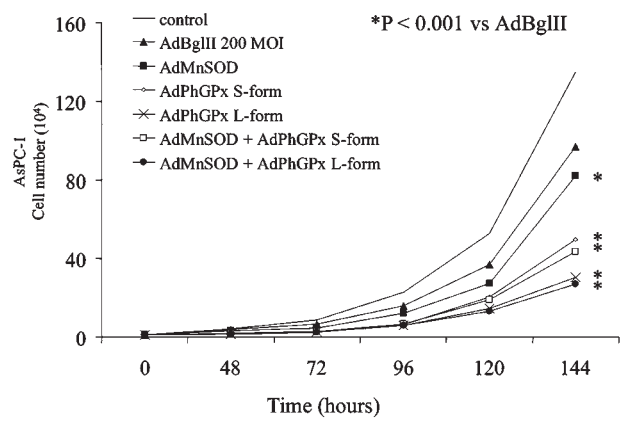
B.



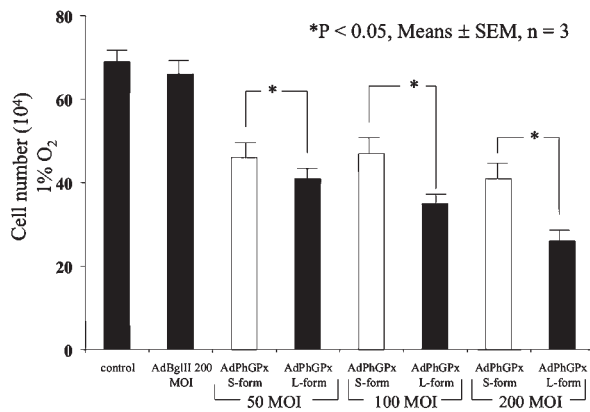
C.



D.



E.



constructs were delivered as AdMnSOD (100 MOI) plus AdBgIII (100 MOI), AdPhGPx (*S-form* or *L-form*) (100 MOI) plus AdBgIII (100 MOI), and AdPhGPx (*S-form* or *L-form*) (100 MOI) plus AdMnSOD (100 MOI).

Plating efficiency

Cells (2.5×10^2) transduced with AdMnSOD, AdPhGPx, AdMnSOD plus AdPhGPx, or AdBgIII (100 MOI) were plated into 6-well plates in complete medium. The dishes were maintained in the incubator for 10 days to allow colony formation. The colonies were then fixed and stained with 0.1% crystal violet and 2.1% citric acid, and those colonies containing greater than 50 cells were scored.

Anchorage-independent growth in soft agar

Cells (5×10^3) transduced with AdMnSOD, AdPhGPx, AdMnSOD plus AdPhGPx, or AdBgIII were suspended in 3 ml of complete medium containing a solution of 6% agar in double-distilled H₂O so that the final concentration of the agar was 0.3%. This suspension was then plated over 3 ml of complete medium made with a 6% agar solution in double-distilled H₂O so that the final concentration of the bottom agar was 0.5%. After 16 days, colonies greater than 0.1 mm in diameter were

scored. The clonogenic fraction was determined on the basis of the following equation:

$$\text{Soft agar plating efficiency (PE)} = \frac{\text{colonies formed}}{\text{cells seeded}} \times 100\%$$

Nude mice

Thirty-day-old athymic female nude mice were obtained from Harlan (Indianapolis, IN). The nude mouse protocol was reviewed and approved by the Animal Care and Use Committee of the University of Iowa. The animals were housed four to a cage and fed a sterile commercial stock diet and tap water, *ad libitum*. Animals were allowed to acclimate in the unit for 1 week before any manipulations were performed.

In vivo adenovirus experiments

MIA PaCa-2 tumor cells (2×10^6) were delivered subcutaneously into the flank region of nude mice from a 1-cm³ tuberculin syringe equipped with a 25-gauge needle. The tumors were allowed to grow until they reached between 3 and 4 mm in greatest dimension (from 10 days to 2 weeks), at which time they were treated with adenovirus. Two separate *in vivo* studies were performed. Each study consisted of six mice in each experi-

FIG. 2. Cell growth. (A) MIA PaCa-2 cells transduced with 0 to 200 MOI of AdPhGPx-*S-form* or 100 MOI of AdBgIII demonstrated reductions in cell growth with AdPhGPx at 100 and 200 MOI. No significant changes were seen with 100-MOI AdBgIII-infected cells compared with parental cells. Mean *in vitro* cell growth of control, AdPhGPx *S-form*-transduced, and AdBgIII-transduced MIA PaCa-2 cells is shown. Each point represents the mean value, $n = 3$. * $p < 0.05$ versus 100 MOI of AdBgIII. (B) MIA PaCa-2 cells transduced with 0 to 200 MOI of AdPhGPx-*L-form* or 100 MOI of AdBgIII demonstrated reductions in cell growth with AdPhGPx-*L-form* at 100 and 200 MOI. No significant changes were seen with 100-MOI AdBgIII-infected cells compared with parental cells. Mean *in vitro* cell growth of control, AdPhGPx-*L-form*-transduced, and AdBgIII-transduced MIA PaCa-2 cells is shown. Each point represents the mean value, $n = 3$. * $p < 0.05$ versus 100 MOI of AdBgIII. (C) MIA PaCa-2 cells transduced with 100 MOI of AdPhGPx-*S-form*, 100 MOI of AdPhGPx-*L-form*, 100 MOI of AdMnSOD, 100 MOI of AdPhGPx-*S-form* plus 100 MOI of AdMnSOD, or 100 MOI of AdPhGPx-*L-form* plus 100 MOI of AdMnSOD demonstrated significant reductions in growth compared with parental cells and those infected with AdBgIII. No significant changes were seen with AdBgIII-infected cells compared with parental cells. The AdBgIII vector was given to equal the viral load of the combined viruses. Thus, AdBgIII was delivered as 200 MOI, and the other constructs were delivered as AdMnSOD (100 MOI) plus AdBgIII (100 MOI), AdPhGPx-*S-form* or AdPhGPx-*L-form* (100 MOI) plus AdBgIII (100 MOI), and AdPhGPx-*S-form* or AdPhGPx-*L-form* (100 MOI) plus AdMnSOD (100 MOI). AdPhGPx-transduced cells (*S-form* and *L-form*) demonstrated slower *in vitro* growth compared with parental cells or cells infected with AdBgIII. Enforced expression of MnSOD with the AdMnSOD vector also slowed *in vitro* growth compared with parental cells or cells infected with AdBgIII. However, addition of AdMnSOD (100 MOI) did not add to the growth-inhibitory effects of AdPhGPx-*S-form* or AdPhGPx-*L-form* (100 MOI). Mean *in vitro* growth of MIA PaCa-2 cells is shown. Each point represents the mean value, $n = 3$. * $p < 0.001$ versus AdBgIII. (D) AsPC-1 cells transduced with 100 MOI of AdPhGPx-*S-form*, 100 MOI of AdPhGPx-*L-form*, 100 MOI of AdMnSOD, 100 MOI of AdPhGPx-*S-form* plus 100 MOI of AdMnSOD, or 100 MOI of AdPhGPx-*L-form* plus 100 MOI of AdMnSOD demonstrated significant reductions in growth compared with parental cells and those infected with AdBgIII. No significant changes were seen with AdBgIII-infected cells compared with parental cells. Once again the AdBgIII vector was given to equal the viral load of the combined viruses. AdPhGPx-transduced cells (*S-form* and *L-form*) demonstrated slower *in vitro* growth compared with parental cells or cells infected with AdBgIII. As seen with the MIA PaCa-2 cell line, enforced expression of MnSOD with the AdMnSOD vector also slowed *in vitro* growth compared with parental cells or cells infected with AdBgIII. However, addition of AdMnSOD (100 MOI) did not add to the growth-inhibitory effects of AdPhGPx-*S-form* or AdPhGPx-*L-form* (100 MOI). Mean *in vitro* growth of AsPC-1 cells is shown. Each point represents the mean value, $n = 3$. * $p < 0.001$ versus AdBgIII. (E) MIA PaCa-2 cells grown in 1% O₂ and transduced with 100 MOI of AdBgIII or 0 to 200 MOI of AdPhGPx-*S-form* or AdPhGPx-*L-form* demonstrated reductions in cell growth with AdPhGPx at 50, 100, and 200 MOI. No significant changes were seen with AdBgIII transferred at 100 MOI compared with parental cells. AdPhGPx-*L-form* had significant decreases in cell growth compared with cells infected with the AdPhGPx-*S-form* vector. Mean *in vitro* cell growth of control, AdPhGPx-*S-form*-transduced, AdPhGPx-*L-form*-transduced, or AdBgIII-transduced MIA PaCa-2 cells is shown. Each point represents the mean value, $n = 3$. * $p < 0.05$ versus AdPhGPx-*S-form*.

mental group. Experimental groups included controls, AdBglII, AdPhGPx-S-form, and AdPhGPx-L-form. The adenoviral constructs were delivered through two injection sites into the tumor.

Tumor size was measured every 2 to 3 days with vernier calipers, and tumor volume was estimated according to the following formula: tumor volume = $\pi/6 \times L \times W^2$, where L is the greatest dimension of the tumor and W is the dimension of the tumor in the perpendicular direction (Weydert *et al.*, 2003). Animals were killed by CO₂ asphyxiation when the tumors reached a predetermined size of 10 × 10 mm, and this was considered the time to sacrifice.

Statistical analysis

Statistical analysis for the *in vitro* studies was performed with SYSTAT (Systat Software, Point Richmond, CA). Single-factor analysis of variance (ANOVA), followed by post-hoc Tukey test, was used to determine statistical differences between means. All means were calculated from three experiments, and error bars represent the standard error of the mean (SEM). All Western blots, immunoblots, activity assays, and activity gel assays were repeated at least twice. Statistical analyses of the *in vivo* studies focused on the effects of the different treatment strategies on cancer progression. The primary outcomes of interest were time to death and tumor growth over time. MIA PaCa-2 tumor cells (2×10^6) were injected into the flanks of nude mice at the start of each study. When the tumors reached visible size, the mice were then randomly assigned to a treatment group and monitored until death or until the experiment was terminated. Tumor sizes (mm³) were periodically measured throughout the experiments, resulting in repeated measurements across time for each mouse. Mixed linear regression models were used to estimate and compare the group-specific tumor growth curves. In both the survival and growth curve analyses, statistically significant global tests of equality across groups were followed up with pairwise comparisons to identify specific group differences. Kaplan–Meier survival plots were constructed to estimate the survival functions. All tests were two-sided and carried out at the 5% level of significance. Analyses were performed with the SAS (Cary, NC) and R statistical software packages.

RESULTS

Western analysis of PhGPx in normal pancreas and pancreatic tumor cell lines

PhGPx immunoreactivity was increased in normal human pancreas when compared with the poorly to undifferentiated primary pancreatic tumor cell lines AsPC-1 (0.5), MIA PaCa-2 (0.35), Panc-1 (0.4), and BxPC-3 (0.45) (Fig. 1A). Normal pancreas was observed to have two major bands of immunoreactive protein. The significance of this is not understood. Both forms of PhGPx have been reported to be processed to the same molecular mass, so only one band should be observed. Perhaps some form of post-translational modification occurs in normal pancreas tissue.

Adenovirus gene transfer

Western analysis. A dose-dependent increase in PhGPx immunoreactivity was observed in MIA PaCa-2 cells infected with

both the *PhGPx-S-form* and *PhGPx-L-form* constructs (Fig. 1B and C). PhGPx immunoreactivity was similar in parental cells and cells transduced with AdBglII at 200 MOI. Densitometric analysis demonstrated that the amount of immunoreactive protein was increased over that of AdBglII cells by 3-fold in 200-MOI AdPhGPx-S-form-transduced cells (Fig. 1B) and increased 2.4-fold in 200-MOI AdPhGPx-L-form-transduced cells (Fig. 1C). Infection with AdPhGPx-S-form led to two bands on the Western blot, whereas only one band was seen for control and AdBglII-transduced cells. It is tempting to speculate that the bottom band is PhGPx S-form and the top band is PhGPx L-form. However, both PhGPx forms have been reported to have the same molecular mass. Moreover, PhGPx L-form is not found in appreciable amounts in most cells. Thus, it seems likely that both bands in Fig. 1B are PhGPx S-form and we have quantitated the data accordingly. An increase in MnSOD immunoreactivity was observed in cells transfected with 100 MOI of the AdMnSOD construct (Fig. 1D). MnSOD immunoreactivity was similar in parental and 100-MOI AdBglII-transduced cells (Fig. 1D). Densitometric analysis demonstrated that the amount of immunoreactive protein was increased by nearly 9-fold in 100-MOI AdMnSOD-transduced cells compared with AdBglII cells.

Tumor biological characteristics of adenovirus-transduced cells

Cell growth. MIA PaCa-2 pancreatic cancer cells transduced with either AdPhGPx-S-form or AdPhGPx-L-form demonstrated slower *in vitro* growth compared with parental cells or cells infected with AdBglII (Fig. 2). Tumor cell-doubling time was 20.8 ± 0.8 and 22.7 ± 0.8 hr (means \pm SEM) for the parental cell line and AdBglII-infected cells, respectively. The doubling time increased significantly to 25.9 ± 1.1 and 30.3 ± 2.2 hr with the 100- and 200-MOI doses of AdPhGPx-S-form, respectively (both $p < 0.05$ versus AdBglII) (Fig. 2A). For example, on day 7, cell number decreased by 51% with AdPhGPx-S-form at 100 MOI, and decreased by 72% with AdPhGPx-S-form at 200 MOI compared with MIA PaCa-2 cells transduced with AdBglII at 100 MOI (Fig. 2A). AdPhGPx-L-form appeared to have an even greater effect in inhibiting tumor cell growth. Tumor cell-doubling time increased significantly to 33.9 ± 1.2 and 46.5 ± 2.7 hr (means \pm SEM) with the 100- and 200-MOI doses of AdPhGPx-L-form, respectively (both $p < 0.05$ versus AdBglII) (Fig. 2B). For example, on day 7, cell number decreased by 78% with AdPhGPx-L-form at 100 MOI, and decreased by 92% with AdPhGPx-L-form at 200 MOI compared with MIA PaCa-2 cells transduced with AdBglII at 100 MOI (Fig. 2B).

Previous studies in pancreatic cancer have demonstrated that MnSOD overexpression suppresses tumor growth, both *in vitro* and *in vivo* (Cullen *et al.*, 2003b; Weydert *et al.*, 2003). Previous studies from our laboratory also demonstrated that the tumor-suppressive effect of MnSOD overexpression in pancreatic cancer was enhanced by increasing peroxide removal by overexpression of GPx1 (Liu *et al.*, 2004). Thus, we wanted to determine whether the same phenomenon occurred with PhGPx overexpression. To equalize the viral load of the combined viruses in these experiments, the AdBglII vector was given. For example, 100 MOI of AdPhGPx (S-form or L-form) was given along with 100 MOI of AdBglII to equal the viral load of the

combination of AdPhGPx (100 MOI) plus AdMnSOD (100 MOI). In a separate study, AdPhGPx-*S-form*-transduced cells once again demonstrated slower *in vitro* growth compared with parental cells or cells infected with AdBgIII at 200 MOI ($p < 0.05$ versus AdBgIII, means \pm SEM) (Fig. 2C). Enforced expression of MnSOD with the AdMnSOD vector also slowed *in vitro* growth compared with parental cells or cells infected with AdBgIII at 200 MOI ($p < 0.05$ versus AdBgIII, means \pm SEM). However, the combination of AdPhGPx-*S-form* (100 MOI) and AdMnSOD (100 MOI) did not add to the inhibition of cell growth with AdPhGPx-*S-form* alone (Fig. 2C). Likewise, the combination of AdPhGPx-*L-form* (100 MOI) and AdMnSOD (100 MOI) did not add to the inhibition of cell growth with the AdPhGPx-*L-form* vector alone (Fig. 2C). To determine whether the inhibition in cell growth demonstrated with overexpression of PhGPx was unique to one particular pancreatic cancer cell line, we repeated the cell growth study in another pancreatic cancer cell line, AsPC-1 (Fig. 2D). Once again, AdPhGPx-transduced cells (*S-form* and *L-form*) demonstrated slower *in vitro* growth compared with parental cells or cells infected with AdBgIII. Enforced expression of MnSOD with the AdMnSOD vector also slowed *in vitro* growth compared with parental cells or cells infected with AdBgIII. However, the addition of AdMnSOD (100 MOI) did not add to the growth-inhibitory effects of AdPhGPx-*S-form* or AdPhGPx-*L-form* (100 MOI). The rest of the *in vitro* and *in vivo* studies were performed in the MIA PaCa-2 cell line.

The previous growth experiments were performed in 21% O₂. To determine whether enforced expression of PhGPx would have the same growth-inhibitory effect in the hypoxic environment of pancreatic tumors, growth was determined in cells grown in 1% O₂. In MIA PaCa-2 cells infected with AdPhGPx-*S-form* (50, 100, or 200 MOI), there was a 32% decrease in cell number on day 17 compared with either control cells or those infected with AdBgIII at 200 MOI (Fig. 2E) ($p < 0.05$ versus AdBgIII). Likewise, in pancreatic cancer cells infected with AdPhGPx-*L-form* (50, 100, or 200 MOI), there was a 63% decrease in cell number on day 17 compared with either control cells or those infected with AdBgIII at 200 MOI ($p < 0.05$ versus AdBgIII). Also, the AdPhGPx-*L-form* vector, which is targeted to the mitochondria, had a significantly greater effect in inhibiting growth when compared with AdPhGPx-*S-form* and given at the same MOI ($p < 0.05$).

Plating efficiency. To determine the clonogenic capacity of cells transduced with AdPhGPx (*S-form* and *L-form*), we performed a plating efficiency assay. In general, malignant cells have a higher plating efficiency than normal cells. Cells transduced with AdPhGPx (both *S-form* and *L-form*) demonstrated a dose-dependent decreased plating efficiency compared with parental cells or cells infected with AdBgIII. MIA PaCa-2 plating efficiency significantly decreased with AdPhGPx-*S-form* (100–200 MOI) when compared with parental cells or 100-MOI

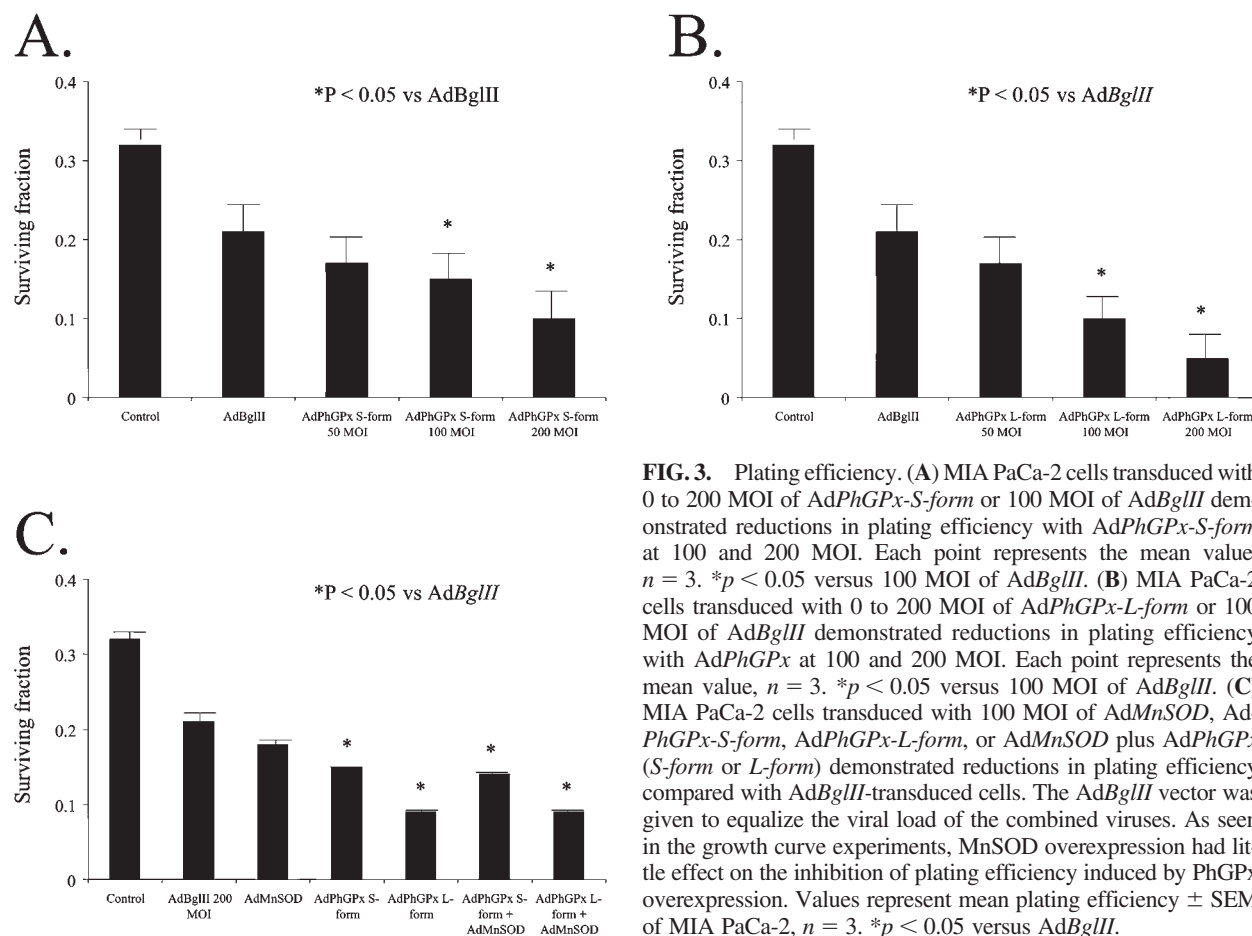


FIG. 3. Plating efficiency. (A) MIA PaCa-2 cells transduced with 0 to 200 MOI of AdPhGPx-*S-form* or 100 MOI of AdBgIII demonstrated reductions in plating efficiency with AdPhGPx-*S-form* at 100 and 200 MOI. Each point represents the mean value, $n = 3$. * $p < 0.05$ versus 100 MOI of AdBgIII. (B) MIA PaCa-2 cells transduced with 0 to 200 MOI of AdPhGPx-*L-form* or 100 MOI of AdBgIII demonstrated reductions in plating efficiency with AdPhGPx at 100 and 200 MOI. Each point represents the mean value, $n = 3$. * $p < 0.05$ versus 100 MOI of AdBgIII. (C) MIA PaCa-2 cells transduced with 100 MOI of AdMnSOD, AdPhGPx-*S-form*, AdPhGPx-*L-form*, or AdMnSOD plus AdPhGPx (*S-form* or *L-form*) demonstrated reductions in plating efficiency compared with AdBgIII-transduced cells. The AdBgIII vector was given to equalize the viral load of the combined viruses. As seen in the growth curve experiments, MnSOD overexpression had little effect on the inhibition of plating efficiency induced by PhGPx overexpression. Values represent mean plating efficiency \pm SEM of MIA PaCa-2, $n = 3$. * $p < 0.05$ versus AdBgIII.

AdBgIII cells (Fig. 3A). Plating efficiency was $21 \pm 1\%$ in AdBgIII-transfected cells, which decreased to 15 ± 1 and $10 \pm 1\%$ in cells transfected with AdPhGPx-S-form at 100 and 200 MOI, respectively (both $p < 0.05$ versus AdBgIII at 200 MOI). As seen in the growth curve experiments, overexpression of AdPhGPx-L-form seemed to have an even greater inhibitory effect on plating efficiency (Fig. 3B). As mentioned, plating efficiency was $21 \pm 1\%$ in AdBgIII-transfected cells, which decreased to 10 ± 1 and $5 \pm 1\%$ in cells transfected with AdPhGPx-L-form at 100 and 200 MOI, respectively (both $p < 0.05$ versus AdBgIII).

To determine whether overexpression of PhGPx would potentiate the plating efficiency-suppressive effect of MnSOD overexpression, we performed a separate study. As in the cell growth experiments, AdBgIII vector was given to equalize the viral load of the combined viruses (Fig. 3C). Thus, 100 MOI of AdPhGPx (S-form or L-form) was given along with 100 MOI of AdBgIII to equal the viral load of the combination of AdPhGPx (100 MOI) plus AdMnSOD (100 MOI). As seen in the growth curve experiments, the addition of MnSOD overexpression had little effect on the inhibition of plating efficiency induced by PhGPx overexpression (Fig. 3C) ($p > 0.05$).

Growth in soft agar. To examine anchorage-dependent growth, we performed a soft agar assay. Whereas malignant cells form colonies in soft agar, normal cells do so in far smaller numbers. MIA PaCa-2 soft agar plating efficiency significantly decreased with AdPhGPx-S-form (50, 100, and 200 MOI) when compared with parental cells or 200-MOI AdBgIII cells (Fig. 4A). Soft agar plating efficiency was reduced by 69, 61, and 81% with 50-, 100-, and 200-MOI doses of AdPhGPx-S-form, respectively (all $p < 0.05$ versus AdBgIII). Likewise, soft agar plating efficiency was reduced by 63, 60, and 65% with 50-, 100-, and 200-MOI doses of AdPhGPx-L-form, respectively (all $p < 0.05$ versus AdBgIII) (Fig. 4B). The reductions in soft agar growth were not dose dependent as seen in the plating efficiency experiments, suggesting that the 50-MOI dose may have maximum effects in soft agar and that increasing the dose will not result in further inhibition of growth. As seen in both the growth curve and plating efficiency experiments, enforced expression of MnSOD did not have an additive effect in the PhGPx-induced decrease in soft agar growth (data not shown).

In vivo studies

Our *in vitro* results demonstrate that both PhGPx S-form and PhGPx L-form significantly inhibit pancreatic cancer cell growth. To determine the *in vivo* effects of these antioxidant enzymes, MIA PaCa-2 pancreatic cancer cells were injected into the flanks of nude mice and the tumors were allowed to grow until they were 3–4 mm in diameter. At that time, the adenoviral constructs were injected intratumorally. Four groups of mice consisting of 6 mice in each group included controls (3% sucrose), AdBgIII, AdPhGPx-S-form, and AdPhGPx-L-form (Fig. 5A). To compare the treatment groups over time for tumor volume, mixed linear regression analysis was used (Liang and Zeger, 1986). Table 1 summarizes the results from the mixed linear regression analysis of the tumor growth curves. The sample sizes given in Table 1 are the total number of measurements available within each group. The p value is for the

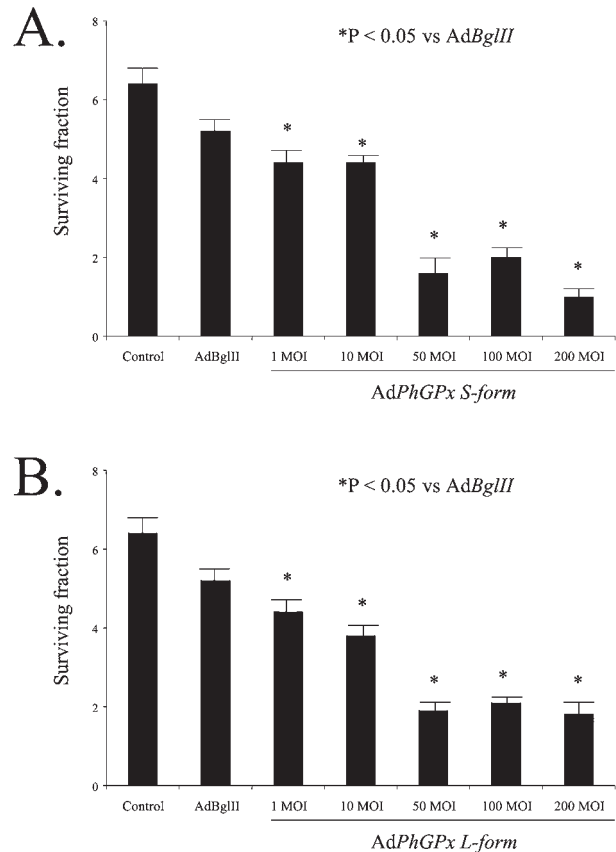


FIG. 4. Growth in soft agar. (A) MIA PaCa-2 cells transduced with 0 to 200 MOI of AdPhGPx-S-form or 100 MOI of AdBgIII demonstrated reductions in soft agar growth with AdPhGPx-S-form at 1–200 MOI. Mean *in vitro* soft agar growth of control, AdPhGPx-transduced, or AdBgIII-transduced MIA PaCa-2 cells is shown. Each point represents the mean value, $n = 3$. * $p < 0.05$ versus 100 MOI of AdBgIII. (B) MIA PaCa-2 cells transduced with 0 to 200 MOI of AdPhGPx-L-form or 100 MOI of AdBgIII demonstrated reductions in soft agar growth with AdPhGPx-L-form at 1–200 MOI. Mean *in vitro* soft agar growth of control, AdPhGPx-transduced, or AdBgIII-transduced MIA PaCa-2 cells is shown. Each point represents the mean value, $n = 3$. * $p < 0.05$ versus 100 MOI of AdBgIII.

global tests of equality between the growth curves across treatment groups. There was a significant difference between the curves ($p < 0.0001$). Pairwise group comparisons were carried out to identify where the group differences occurred. Groups for which there was no difference at the 5% level of significance appear together. There was no significant difference between controls and the AdBgIII-treated animals, between controls and animals treated with AdPhGPx-S-form, and between the AdBgIII group and the AdPhGPx-S-form group. However, animals treated with AdPhGPx-L-form were significantly different from the control, AdBgIII, and AdPhGPx-S-form groups ($p < 0.0001$ for each comparison). For example, tumor size was reduced by 66% on day 21 in animals that received a single injection of the AdPhGPx-L-form vector when compared with animals with pancreatic tumors treated with AdBgIII. Likewise, tumor volume was reduced by 32% on day 21 in animals that received a single injection of the AdPhGPx-L-form vector.

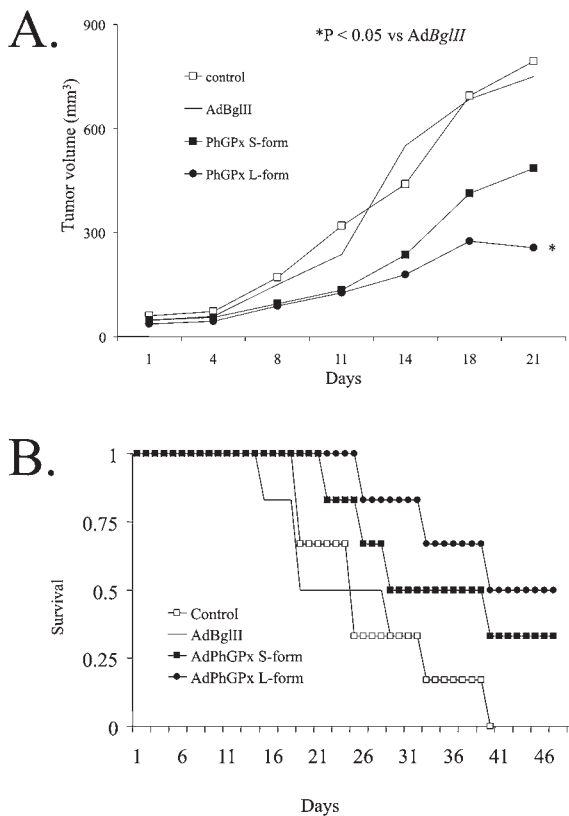


FIG. 5. *In vivo* tumor growth. (A) MIA PaCa-2 tumor cells (2×10^6) were delivered subcutaneously into the flank region of nude mice. Controls received serum-free medium or AdBgIII in similar volumes and plaque-forming units at the same time points. AdPhGPx-S-form or AdPhGPx-L-form (1×10^9 PFU) was delivered to the tumor on day 1 of the experiment. AdPhGPx-L-form injections decreased MIA PaCa-2 tumor growth in nude mice ($n = 6$ per group, mean tumor volume, $p < 0.0001$). Pairwise comparisons were not significantly different when comparing serum-free medium (controls) with the groups of animals that received the AdBgIII or AdPhGPx-S-form vector. (B) Kaplan–Meier plots of estimated survival after injection of MIA PaCa-2 tumors into nude mice. There was a significant difference between controls and AdPhGPx-L-form-treated animals ($p = 0.03$) and between the AdBgIII group and AdPhGPx-L-form-treated animals ($p = 0.02$).

The global test of equality indicated that there was a significant difference in survival time in the first *in vivo* xenograft study ($p = 0.03$) (Fig. 5B). No significant difference was observed between controls (median survival, 25 days), AdBgIII-treated animals (median survival, 23 days), and AdPhGPx-S-form-treated animals (median survival, 33.5 days). However, there was a significant difference between controls and AdPhGPx-L-form-treated animals (median survival, 42.5 days) ($p = 0.03$) and between the AdBgIII group and AdPhGPx-L-form-treated animals ($p = 0.02$).

In the second *in vivo* study, four groups of mice were once again used, consisting of six mice in each group, including controls (3% sucrose), AdBgIII, AdPhGPx-S-form, and AdPhGPx-L-form. In contrast to the first *in vivo* study, tumor volume was 40–50% larger when treatment was begun (Fig. 6A). Table 2

summarizes the results from the mixed linear regression analysis of the tumor growth curves. The sample sizes given in Table 2 are the total number of measurements available within each group. The rate of growth did not differ significantly between the groups ($p = 0.16$). However, results of the mixed linear regression models comparing tumor growth between the group of animals that received AdBgIII was significantly different from that of the group of animals receiving AdPhGPx-L-form ($p = 0.04$). In fact, tumor volume was reduced by 32% on day 21 in animals that received a single injection of the AdPhGPx-L-form vector. Although mice treated with the AdPhGPx-L-form vector had the longest survival, there were no significant differences in survival among the four groups (Fig. 6B).

DISCUSSION

Antioxidant enzymes are highly compartmentalized and generally adequate to prevent toxicity of reactive oxygen species, thereby maintaining cellular homeostasis under normal physiologic conditions. However, levels of antioxidant enzymes in cancer cells are significantly different from those in normal counterpart cells. This reduction in antioxidant enzymes may also lead to malignant transformation. Studies from our laboratory have demonstrated that in human pancreatic carcinoma specimens, cytoplasmic values of GPx1 protein were decreased when compared with normal pancreas (Cullen *et al.*, 2003a). In another study from our laboratory, GPx1 immunoreactivity was decreased in four pancreatic cancer cell lines when compared with normal pancreas (Cullen *et al.*, 2003a). Also, when using native gels to measure GPx activity, GPx activity was present in the human pancreas but decreased in all of the pancreatic cancer cell lines studied. Thus, in both human pancreatic cancer specimens and human pancreatic cancer cell lines, GPx levels are lower than in normal pancreas. Although our present study suggests that PhGPx levels are also lower in pancreatic cancer than in normal pancreas, our samples of normal pancreas may contain various cell types whereas our pancreatic cancer cell lines all arise from the ductal epithelium. Although we used normal human pancreas from heart-beating transplant donors as our controls, the human pancreas contains numerous

TABLE 1. RESULTS OF MIXED LINEAR REGRESSION MODELS COMPARING TUMOR GROWTH BETWEEN TREATMENT GROUPS FOR DATA SHOWN IN FIGURE 5A^a

Group	n	Mean tumor size (mm)	p Value
Control	49	424.8	
AdBgIII	46	363.3	
AdPhGPx-S-form	59	324.0	
AdPhGPx-L-form	65	223.9	<0.0001 ^b

^aThe sample sizes given represent the total number of measurements available within each group. The p value is for the global test of equality across groups. Group comparisons indicate differences between specific groups at the 5% level of significance.

^bAnimals treated with AdPhGPx-L-form were significantly different from control animals and animals treated with AdBgIII and AdPhGPx-S-form ($p < 0.0001$ for each comparison).

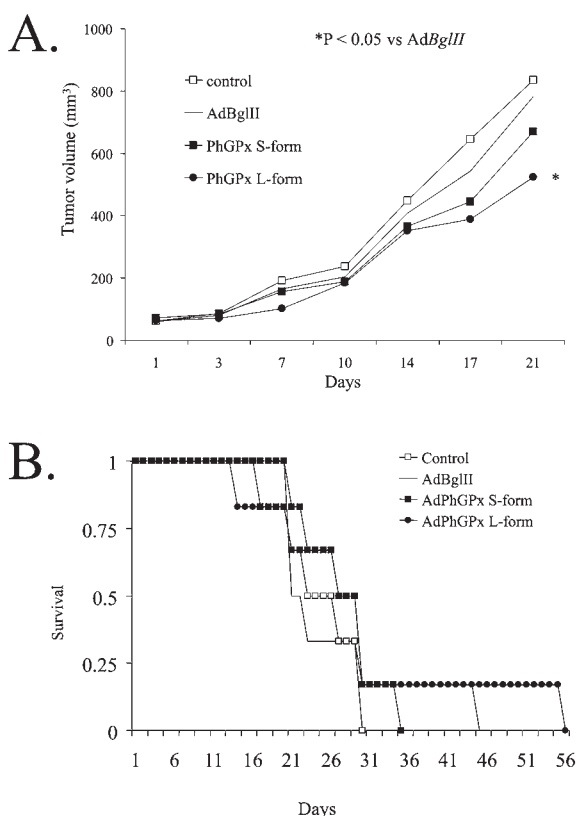


FIG. 6. *In vivo* tumor growth. (A) MIA PaCa-2 tumor cells (2×10^6) were delivered subcutaneously into the flank region of nude mice. Controls received serum-free medium or AdBgIII in similar volumes and plaque-forming units at the same time points. AdPhGPx-S-form or AdPhGPx-L-form (1×10^9 PFU) was delivered to the tumor on day 1 of the experiment. Results of the mixed linear regression models demonstrated that tumor growth was significantly decreased in the group of animals that received AdPhGPx-L-form compared with the group of animals that received AdBgIII. (B) Kaplan–Meier plots of estimated survival after injection of MIA PaCa-2 tumors into nude mice. There were no differences in time to sacrifice between the four groups of mice.

cell types. Further studies will need to be performed to confirm altered PhGPx levels in pancreatic cancer.

Our group demonstrated that in human pancreatic cancer cells that overexpress Ras, overexpression of GPx with an adenoviral vector carrying the *GPx1* gene slowed cell growth and decreased plating efficiency and growth in soft agar, whereas GPx overexpression combined with overexpression of MnSOD had the greatest effect on pancreatic tumor cell growth suppression (Liu *et al.*, 2004). *In vivo*, either GPx1 or MnSOD alone slowed pancreatic tumor growth in nude mice, whereas the combination of AdGPx1 and AdMnSOD potentiated tumor growth suppression and increased animal survival. Our current study demonstrates that an adenoviral vector carrying either the *PhGPx-S-form* gene or *PhGPx-L-form* gene suppressed pancreatic tumor growth; however, the addition of MnSOD overexpression had little effect compared with PhGPx overexpression alone. The reason for a lack of additive effect of MnSOD with PhGPx is puzzling. One explanation is that the two proteins are in different subcellular

locations, so that they do not interact. Another explanation is that peroxidized phospholipids stimulate pancreatic cancer cell growth. GPx1 acts with high efficiency on hydrogen peroxide, but with low efficiency on membrane-bound lipid peroxides, whereas PhGPx can directly reduce peroxidized phospholipid and cholesterol in membranes (Aumann *et al.*, 1997). If PhGPx is more efficient in reducing oxidized phospholipids, and oxidized phospholipids can cause cell proliferation, the addition of MnSOD is not beneficial because it may not affect the levels of oxidated phospholipids and thus the reduction in cell proliferation cannot be increased further.

Thus, inhibition of pancreatic cancer cell growth by the removal of hydroperoxides by PhGPx may be due to lipid hydroperoxides generated from lipid membranes, which are precursors to metabolites that increase proliferation. As mentioned, multiple lines of evidence have linked pancreatic cancer growth with lipid content. The pathways involved in the conversion of the unsaturated fatty acids to their bioactive lipid metabolites appear to be involved in the development and growth of multiple human cancers. Several pathways exist in the metabolism of arachidonic and linoleic acid, which are derived from membrane phospholipids by the action of phospholipase A₂ (Ding *et al.*, 1999a,b). Lipoxygenases then act on arachidonic acid to produce hydroperoxy-eicosatetraenoic acid (HPETE) and appear to be important in the development of human pancreatic cancer (Ding *et al.*, 2001).

The formation of superoxide in the respiratory chain takes place spontaneously in the electron-rich area near the inner mitochondrial membrane. Superoxide radicals are readily dismutated by MnSOD and CuZnSOD, leading to the production of hydrogen peroxide. In mitochondria, there are many electron transport enzymes containing Fe–S centers. The reaction between H₂O₂ and Fe²⁺ can lead to HO[•] production via the Fenton reaction. Hydroxyl radicals can trigger chain lipid peroxidation by abstracting a hydrogen atom from unsaturated fatty acids of the membrane, leading to the generation of lipid radicals, which then combine with molecular oxygen. The radicals formed then propagate the chain of lipid peroxidation. The mitochondrial membrane components are rich in phospholipid and unsaturated fatty acids that are particularly susceptible to oxygen radical attack, supporting the role of PhGPx L-form in growth inhibition. Other membrane components could also be susceptible to free radicals, consistent with our findings with PhGPx S-form. Because PhGPx is a unique intracellular antioxidant enzyme that directly reduces

TABLE 2. RESULTS OF MIXED LINEAR REGRESSION MODELS COMPARING TUMOR GROWTH BETWEEN TREATMENT GROUPS FOR DATA SHOWN IN FIGURE 6A^a

Group	n	Mean tumor size (mm ³)	p Value ^b
Control	51	456.6	
AdBgIII	52	391.1	0.16
AdPhGPx-S-form	55	423.8	0.16
AdPhGPx-L-form	54	286.1	0.04

^aThe sample sizes given represent the total number of measurements available within each group. The *p* value is for the global tests of equality across groups.

^bAnimals treated with AdPhGPx-L-form were significantly different from animals treated with AdBgIII (*p* = 0.04).

peroxidized lipids that have been produced in cell membranes, it is responsible for the protection of membranes against oxidative damage (Thomas *et al.*, 1990).

Because of the difference in location, mitochondrial PhGPx (L-form) may prevent changes in mitochondrial functions by reducing intracellular hydroperoxides more efficiently than nonmitochondrial PhGPx (S-form). Arai *et al.* found that overexpression of L-form PhGPx altered cellular function caused by chemical hypoxia induced by exposure to mitochondrial respiratory inhibitors (Arai *et al.*, 1990), and overexpression of L-form PhGPx in a breast tumor epithelial cell line, COH-BR1, altered photochemically generated cholesterol hydroperoxide-induced cell function (Hurst *et al.*, 2001). These findings suggest that the L-form PhGPx may be important in altering mitochondrial function.

Surgical resection of the primary tumor remains the only potentially curative treatment for pancreatic cancer, leading a number of investigators to study other strategies to convert locally unresectable pancreatic cancer to resectable disease. In patients with locally advanced, unresectable pancreatic cancer treated with preoperative chemoradiation therapy to enhance resectability, only 8–12% of patients were able to undergo resection (Jessup *et al.*, 1993; White *et al.*, 1999). Thus, it is unlikely that neoadjuvant chemoradiation can convert unresectable lesions to resectable ones and thereby increase the number of patients who can be cured with combined-modality therapy. Our study presents an attractive alternative in the treatment of pancreatic tumors that at first seem unresectable, by directly injecting an adenoviral vector carrying the *PhGPx* L-form gene to reduce tumor size. Effectiveness of *in situ* gene delivery using adenoviral vectors has been demonstrated, with some investigators reporting gene transfer efficiencies as high as 50% (Chen *et al.*, 1994).

In summary, enforced expression of PhGPx inhibited pancreatic cancer cell growth, and intratumoral injections of the same adenoviral vectors slowed *in vivo* tumor growth and increased animal survival. In all of the studies performed, the *PhGPx* gene targeted to the mitochondria appeared to have a greater pancreatic tumor growth-inhibitory effect than the *PhGPx* gene targeted to the cytosol. Because of the growth-inhibitory effects of PhGPx, lipid hydroperoxides may play an important role in the growth of pancreatic cancer.

ACKNOWLEDGMENTS

Supported by NIH grants DK 60618 and CA 66081, by the Susan L. Bader Pancreatic Cancer Research Fund, and the Medical Research Service, Department of Veterans Affairs.

REFERENCES

- ARAI, M., IMAI, H., and KOUMURA, T. (1990). Mitochondrial phospholipid hydroperoxide glutathione peroxidase plays a major role in preventing oxidative injury to cells. *J. Biol. Chem.* **274**, 4924–4933.
- AUMANN, K.D., BEDORF, N., BRIGELIUS-FLOHE, R., SCHOMBURG, D., and FLOHE, L. (1997). Glutathione peroxidase revisited: Simulation of the catalytic cycle by computer-assisted molecular modelling. *Biomed. Environ. Sci.* **10**, 136–155.
- BRAMHALL, S.R., ALLUM, W.H., and JONES, A.G. (1995). Treatment and survival in 13,560 patients with pancreatic cancer, and incidence of the disease, in the epidemiological study. *Br. J. Surg.* **82**, 111–115.
- CHEN, S.H., SHINE, H.D., GOODMAN, J.C., GROSSMAN, R.G., and WOO, S.L. (1994). Gene therapy for brain tumors: Regression of experimental gliomas by adenovirus-mediated gene transfer *in vivo*. *Proc. Natl. Acad. Sci. U.S.A.* **91**, 3054–3057.
- CULLEN, J.J., MITROS, F.A., and OBERLEY, L.W. (2003a). Expression of antioxidant enzymes in diseases of the human pancreas: Another link between chronic pancreatitis and pancreatic cancer. *Pancreas* **26**, 23–27.
- CULLEN, J.J., WEYDERT, C.A., and HINKHOUSE, M.M. (2003b). The role of manganese superoxide dismutase in the growth of pancreatic adenocarcinoma. *Cancer Res.* **63**, 1297–1303.
- DING, X.Z., IVERSEN, P., CLUCK, M.W., KNEZETIC, J.A., and ADRIAN, T.E. (1999a). Lipoxygenase inhibitors abolish proliferation of human pancreatic cancer cells. *Biochem. Biophys. Res. Commun.* **261**, 218–223.
- DING, X.Z., KUSZYNSKI, C.A., EL-METWALLY, T.H., and ADRIAN, T.E. (1999b). Lipoxygenase inhibition induced apoptosis, morphological changes, and carbonic anhydrase expression in human pancreatic cancer cells. *Biochem. Biophys. Res. Commun.* **266**, 392–399.
- DING, X.Z., TONG, W.G., and ADRIAN, T.E. (2001). 12-Lipoxygenase metabolite 12(S)-HETE stimulates human pancreatic cancer cell proliferation via protein tyrosine phosphorylation and ERK activation. *Int. J. Cancer* **94**, 630–636.
- HURST, R., KORYTOWSKI, W., KRISKA, T., ESWORTHY, R.S., CHU, F.F., and GIROTTI, A.W. (2001). Hyperresistance to cholesterol hydroperoxide-induced peroxidative injury and apoptotic death in a tumor cell line that overexpresses glutathione peroxidase isotype-4. *Free Radic. Biol. Med.* **31**, 1051–1065.
- IMAI, H., and NAKAGAWA, Y. (2003). Biological significance of phospholipid hydroperoxide glutathione peroxidase (PhGPx, Gpx4) in mammalian cells. *Free Radic. Biol. Med.* **34**, 145–169.
- JEMAL, A., TIWARI, R.C., and MURRAY, T., (2004). Cancer statistics, 2004. *CA Cancer J. Clin.* **54**, 8–29.
- JESSUP, J.M., STEELE, G., and MAYER, R.J., (1993). Neoadjuvant therapy for unresectable pancreatic adenocarcinoma. *Arch. Surg.* **128**, 559–564.
- LAM, E.W.N., ZWACKA, R., ENGELHARDT, J.F., DAVIDSON, B.L., DOMANN, F.E., and OBERLEY, L.W. (1997). Adenovirus-mediated manganese superoxide dismutase gene transfer to hamster cheek pouch carcinoma cells. *Cancer Res.* **57**, 5550–5556.
- LIANG, K.-Y., and ZEGER, S.L. (1986). Longitudinal data analysis using generalized linear models. *Biometrics* **73**, 13–22.
- LIU, J., HINKHOUSE, M.M., and SUN, W. (2004). Redox regulation of pancreatic cancer cell growth: Role of glutathione peroxidase in the suppression of the malignant phenotype. *Hum. Gene Ther.* **15**, 239–250.
- OBERLEY, T.D., OBERLEY, L.W., SLATTERY, A.F., LAUCHNER, L.J., and ELWELL, J.H. (1990). Immunohistochemical localization of antioxidant enzymes in adult Syrian hamster tissues and during kidney development. *Am. J. Pathol.* **137**, 199–214.
- SUNDE, R., DYER, J., MORAN, T., EVENSON, J., and SUGIMOTO, M. (1993). Phospholipid hydroperoxide glutathione peroxidase: Full-length pig blastocyst cDNA sequence and regulation by selenium status. *Biochem. Biophys. Res. Commun.* **193**, 905–911.
- THOMAS, J.P., MAIORINO, M., URSINI, F., and GIROTTI, A.W. (1990). Protective action of phospholipid hydroperoxide glutathione peroxidase against membrane-damaging lipid peroxidation: *In situ* reduction of phospholipid and cholesterol hydroperoxides. *J. Biol. Chem.* **265**, 454–461.
- URSINI, F., MAIORINO, M., and ROVERI, A. (1997). Phospholipid hydroperoxide glutathione peroxidase (PhGPx): More than an antioxidant enzyme? *Biomed. Environ. Sci.* **10**, 327–332.

- WEYDERT, C., ROLIING, B., and LIU, J. (2003). Suppression of the malignant phenotype in human pancreatic cancer cells by the over-expression of manganese superoxide dismutase. *Mol. Cancer Ther.* **2**, 361–369.
- WHITE, R., LEE, C., and ANSCHER, M. (1999). Preoperative chemoradiation for patients with locally advanced adenocarcinoma of the pancreas. *Ann. Surg. Oncol.* **6**, 38–45.
- YEO, C.J., and CAMERON, J.L. (1999). Pancreatic cancer. *Curr. Probl. Surg.* **36**, 59–152.
- ZWACKA, R.M., DUDUS, L., EPPERLY, M.W., GREENBERGER, J.S., and ENGELHARDT, J.F. (1998). Redox gene therapy protects human IB-3 lung epithelial cells against ionizing radiation-induced apoptosis. *Hum. Gene Ther.* **9**, 1381–1386.

Address reprint requests to:

Dr. Joseph J. Cullen

4605 JCP

University of Iowa Hospitals and Clinics

Iowa City, IA 52242

E-mail: joseph-cullen@uiowa.edu

Received for publication: September 17, 2005; accepted October 27, 2005.

Published online: December 7, 2005.